

Magnetic field induced drastic violation of Wiedemann-Franz law in Dirac semimetal Cd_3As_2

A. Pariari, N. Khan, and P. Mandal

Saha Institute of Nuclear Physics, 1/AF Bidhannagar, Calcutta 700 064, India

(Dated: September 22, 2021)

The journey through the nontrivial band topology beyond the conventional band structure has resulted in the recent discovery of three-dimensional Dirac semimetal phase in Na_3Bi and Cd_3As_2 [1-7]. The bulk state of which is semi-metallic obeying linear energy dispersion, while the surface state is topology protected Fermi arc [1, 2, 8, 9]. Due to the unique band topology, they show different exotic electronic properties of both fundamental and technological interest. From electrical and thermal transport measurements, we have demonstrated a remarkable violation of Wiedemann-Franz law (WFL) under application of magnetic field in Cd_3As_2 and the violation becomes more and more drastic with increasing magnetic field strength. Whereas the validity of WFL is the key feature of Landau Fermi-liquid theory in metal, the notion of quasiparticles is the building block to this theory. This implies that the fundamental concept of Landau quasiparticle no longer holds in Cd_3As_2 in presence of magnetic field. The continuous break down of Landau quasiparticle framework with field introduces a concept of field induced quantum critical point (QCP) as in the case of heavy fermion compounds YbRh_2Si_2 [10], $\text{Sr}_3\text{Ru}_2\text{O}_7$ [11], etc.

Dirac fermionic excitation and topology introduce different exotic electronic properties of solids which are now the subject of considerable research interest in condensed matter physics, both from basic research and application point of view. This unique excitation was first discovered in two-dimensional graphene [12] followed by topological insulator [13, 14] and the parent compounds of iron-based superconductors [15]. Unlike conventional fermionic excitations in metals, the quasiparticle excitation in these systems follows a linear energy dispersion. Recently, the three-dimensional (3D) Dirac semimetal state has been theoretically predicted, in which the semimetallic bulk is the 3D analog of graphene [1, 2, 8, 9]. The 3D Dirac points, where the two Weyl points overlap in momentum space, are protected by the crystal symmetry [1, 2, 8, 9]. Breaking of time reversal symmetry by external magnetic field (B) rearranges the Fermi surface [1, 2].

Following theoretical prediction [1, 2], 3D Dirac semimetal phase has been discovered experimentally in Na_3Bi and Cd_3As_2 [3-7]. So far, the major attentions

have been focused on the electronic properties of Cd_3As_2 for understanding the nature of band structure [16-19]. It has been observed that the Fermi surface of Cd_3As_2 undergoes a change with the application of magnetic field [18]. In case of heavy fermion compounds like YbRh_2Si_2 , the Fermi surface is strongly affected by B [10, 20]. Above a critical field (B_c), the paramagnetic phase is a heavy Fermi liquid with large Fermi surface due to the Kondo effect and the antiferromagnetic phase below B_c is also a mass enhanced Fermi liquid with small Fermi surface [20]. At $B=B_c$, however, a non-Fermi-liquid ground state emerges in the field-induced QCP as T approaches towards zero [10]. This motivated us to investigate whether the concept of Landau Fermi-liquid holds across the Fermi surface reconstruction in presence of magnetic field in Cd_3As_2 , where instead of strong electron-electron correlation, the spin-orbit coupling plays a crucial role [1].

Here, we focus on the electrical and thermal transport properties of Cd_3As_2 single crystal in magnetic field. Figure 1 displays the normalized magnetoresistivity (ρ) at different temperatures. ρ increases almost linearly with increasing field. Even at 300 K and 9 T magnetic field, ρ shows no sign of saturation, and the resistivity ratio $\rho(B)/\rho(0)$ is ~ 3 . With decreasing temperature, the value of $\rho(B)/\rho(0)$ increases rapidly and at 10 K, it is ~ 17.5 at 9 T. Inset of Fig. 1 shows temperature dependence of ρ . ρ does not follow T^2 and linear T dependence at low temperature and high temperature respectively as in the case of normal metal.

In Fig. 2 (a), κ has been plotted as a function of B at some selected temperatures between 20 and 300 K. κ decreases very rapidly with increasing B and tends to saturate at high B which is expected to be the lattice part of thermal conductivity (κ_L). This saturating behaviour is more prominent below 50 K. The inset of Fig. 2 (a) shows temperature dependence of κ . The sharp increase in κ below 50 K also suggests the smaller proportion of electronic thermal conductivity (κ_e) to the total at low temperature. We have fitted the field dependence of thermal conductivity with

$$\kappa = \kappa_L + \frac{\kappa_e}{1 + \mu_T^2 B^2} \quad (1)$$

to separate κ_e from total thermal conductivity κ , where the $B \rightarrow \infty$ limit will give the value of κ_L and μ_T is the thermal mobility [21-24]. At low temperature, the extracted value of κ_L is close to the value of κ at 9 T.

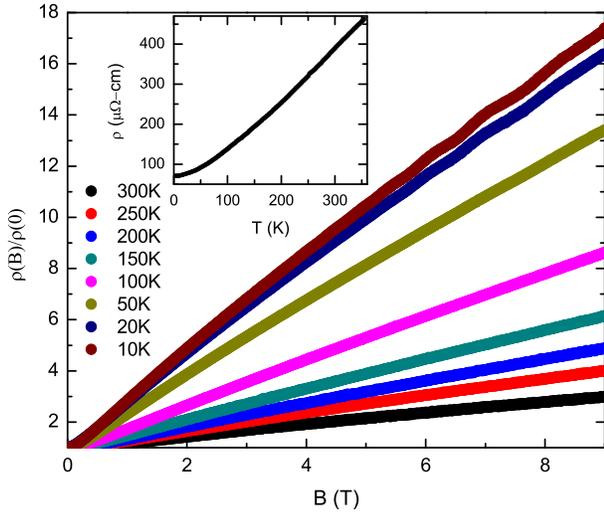


FIG. 1: (color online) Resistivity (ρ) of Cd_3As_2 single crystal in presence of magnetic field at some selected temperatures. Inset shows the temperature dependence of ρ in absence of field.

As an example, at 20 K, we have deduced $\kappa_L = 3.549 \text{ W K}^{-1} \text{ m}^{-1}$ which is close to the observed value of κ at 9 T ($3.55 \text{ W K}^{-1} \text{ m}^{-1}$). If one considers the 1st order expansion of the above equation for $\mu_T B \ll 1$ (for very small B), one finds $\kappa - \kappa_L = \kappa_e(B) = \kappa_e(1 - \mu_T^2 B^2)$. For a 3D Dirac semimetal, the quadratic B of κ_e has been theoretically predicted by considering an energy independent scattering time (τ), which is given by $\kappa_e(B) \propto [1 - (\omega_c \tau)^2]$, where $\omega_c (= eB/\hbar)$ is the cyclotron frequency of the electron orbit [25]. This implies that the above assumption of energy independence of scattering time is not valid at high field.

Below 20 K, instead of showing saturation, κ decreases almost linearly up to 9 T and this effect enhances in the phonon dominated region of κ , as shown in Fig. 2 (b). Now, equation (1) can not be used to separate κ_L from κ . We have measured magnetostriction at low temperature to check whether B induces any structural change. But we have not observed any noticeable changes in lattice parameters. The specific heat does not show any B dependence which implies that the phonon density of state is not affected by B . So, we propose that the observed phenomenon is due to the reduction in lattice thermal conductivity in magnetic field. Recently, the lattice thermal conductivity of diamagnetic semiconductor InSb is reported to exhibit B dependence [26]. In that work, the authors have argued that B creates a spatial gradient in diamagnetic moment around the displaced atoms in phonon vibration which exerts an anharmonic magnetic force on the displaced atom and as a result, a reduction in lattice thermal conductivity. We have estimated about 10% reduction in κ_L at 6 K and 9 T which is comparable to that for InSb [26].

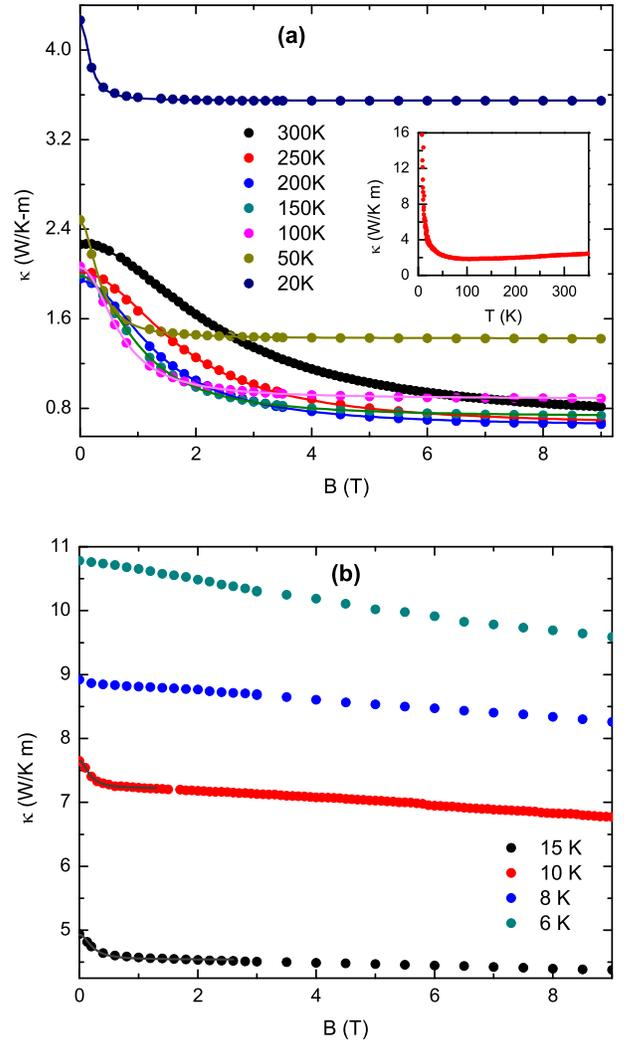


FIG. 2: (color online) Magnetic field dependence of thermal conductivity (a) From 20 to 300K at some representative temperatures up to 9 T. Solid lines are the fitted to the experimental data. Inset shows the temperature dependence of thermal conductivity at zero field. (b) Below 20 K up to 9 T. It has been fitted by equation (1) at 15 and 10 K over a smaller region (solid lines) relative to higher temperatures data.

To calculate $\kappa_e/\sigma T$, i.e., the Lorentz number (L), we have extracted κ_e from κ using equation 1. Figure 3 (a) displays the temperature variation of L in absence of magnetic field. L over most of the temperature range is only about 70% of the ideal value L_0 ($2.44 \times 10^{-8} \text{ W}\Omega\text{K}^{-2}$). L shows a shallow dip around 100 K and approaches rapidly to L_0 at low temperature. Below 10 K, it is difficult to calculate the precise value of L because κ_L is affected by B . The temperature dependence of L is qualitatively similar to earlier report [22], where the B dependence of κ was measured only up to 2 T to separate κ_e using equation 1 and to calculate L .

Figure 3 (b) shows $\kappa_e/\sigma T$ ratio under application

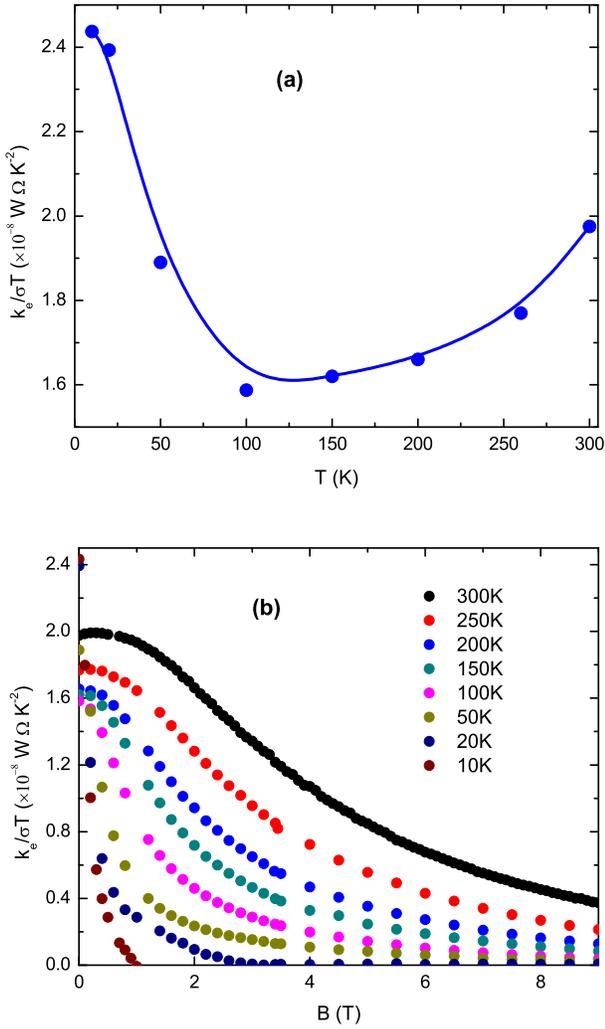


FIG. 3: (color online) (a) Temperature dependence of Lorentz number (L), $\kappa_e/\sigma T$, at zero field. (b) Reduction of $\kappa_e/\sigma T$ ratio under application of magnetic field up to 9 T at some constant temperatures.

of B up to 9 T at some selected temperatures in the range 10 to 300 K. $\kappa_e/\sigma T$ decreases very rapidly with increasing B . At 300 K, it decreases from 1.95 to 0.37 as B increases from zero to 9 T. At low temperatures, however, L reduces more rapidly with increasing field strength. For example, at 20 K, $\kappa_e/\sigma T$ drops from its zero field value 2.39 to ~ 0.006 , only at 3 T. There may be some error in the calculated value of L at 10 K due to smaller proportion of κ_e and the effect of B on κ_L but the qualitative behavior of $L(B)$ remains same. At high fields and low temperature, L is found to be few orders of magnitude smaller than L_0 . This clearly demonstrates a drastic violation of the Wiedemann-Franz law under application of magnetic field in Dirac semimetal Cd_3As_2 . The violation of this universal law can be observed from the non-identical B dependence of κ and σ . $\rho(B)$ does not follow the predicted quadratic B dependence, $\rho(B)/\rho(0) = 1 + \mu_T^2 B^2$, but linear in B

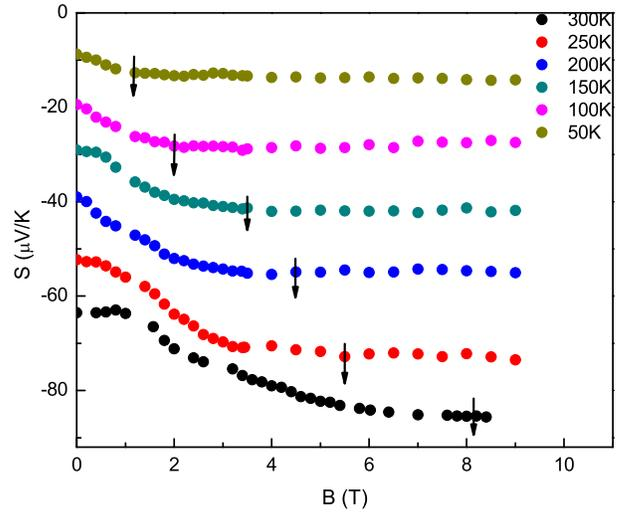


FIG. 4: (color online) Figure shows the effect of magnetic field on Seebeck coefficient (S) up to 9 T at some representative temperatures between 20 to 300 K. Right side of downward arrow represents the value of m close to 1.

[23, 24]. As a result of such unusual linear B dependence of ρ , the ratio $\kappa_e(B)/\sigma(B)$ fails to remain constant.

In order to understand the effect of B on the Fermi surface, we have measured the Seebeck coefficient (S). S increases monotonically with B and tends to saturate at high B as shown in Fig. 4. Also with decreasing temperature, the value of S decreases monotonically and tends to saturate at a relatively lower field strength. The well known Mott's semiclassical formula of thermoelectric power, $S = \frac{\pi^2}{3e} \frac{T}{\sigma(\mu)} \left. \frac{\partial \sigma(\varepsilon)}{\partial \varepsilon} \right|_{\varepsilon=\mu}$, has been used in graphene to probe the relaxation process [27]. Here $\sigma(\varepsilon)$ is energy dependent conductivity, μ is the chemical potential and $\mu = E_F$ for $T \ll T_F$. Using the similar algorithm in case of "3D analog of graphene" and scattering time (τ) $\propto \varepsilon^m$, the above equation simplifies to, $S = \frac{\pi^2 k_B}{3e} \frac{k_B T}{E_F} (m + 2)$. From the linear T dependence of S , we have deduced scattering exponent $m \sim 0.15$ for the relaxation process in Cd_3As_2 single crystal with Fermi energy ~ 270 meV [28]. This linear T dependence of S is robust under application of field (see Supplementary Information). Now, considering the above equation and Fig. 4, it can be shown that m increases monotonically with B and tends to saturate at 1 at high field. Also, it is apparent from Fig. 4 that m reaches close to 1 at lower B with decreasing temperature. The value of m determines the nature of relaxation process of the charge carrier. For examples, $m=2$ for screened charged impurity scattering, $m=-2$ for short-range disorder [25] and for unscreened charged impurity scattering m is 1 [27], etc. The strong B dependence of m can be ascribed to field induced change of Fermi surface, similar to the earlier report [18].

With increasing magnetic field strength, the scattering

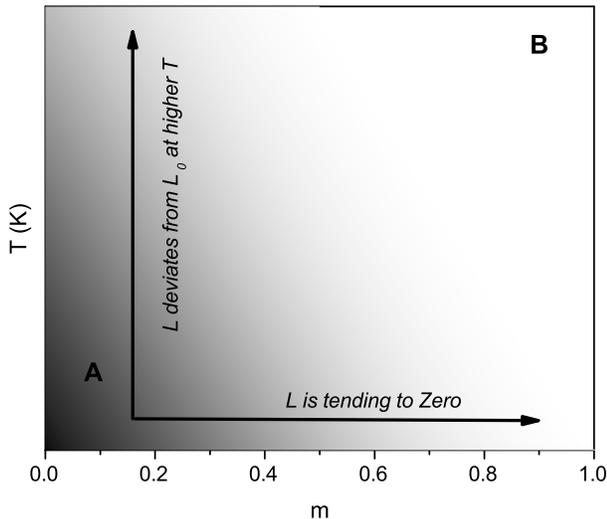


FIG. 5: (color online) A schematic representation. Here, **A** representing the region where the value of Lorentz number (L) is larger than in region **B**. Deeper shaded region represents the value of L closer to L_0 and at $(0,0)$, $L=L_0$. Also it should be noted that there is no sharp boundary between region **A** and **B**. System continuously evolves from region **A** to region **B** with the variation of magnetic field and temperature.

exponents m tends to saturate at 1 while the Lorentz number L falls drastically from its ideal value L_0 . This implies a continuous violation of Wiedemann-Franz law (WFL), i.e, the Landau quasiparticle no longer holds under application of magnetic field. However, the present and earlier studies [22] clearly show that L approaches L_0 at low temperature and zero field. Based on our experimental observation, we have constructed a schematic diagram in Fig. 5. **A** represents the shaded region, where L is closer to L_0 than the value in region **B** and at the origin $(0,0)$, $L=L_0$. The system continuously evolves from **A** to **B** and vice versa with the variation of $m(B)$. Now, by tuning m from ~ 0 to 1 through magnetic field, one observes a continuous breakdown of Landau Fermi liquid behaviour. Thus, $m=1$ looks like a quantum critical point (QCP) at T tends to zero limit. As if, we have been able to achieve the one side of the point. The other side can not be accessed by tuning B as m saturates at 1. Similar kind of behaviour has been observed in heavy fermion compound like YbRh_2Si_2 [10], in which B induces a QCP between paramagnetic heavy Fermi-liquid state and antiferromagnetic mass enhanced Fermi-liquid state, where non-Fermi-Liquid ground state emerges. The present study introduces the concept of field-induced QCP in Dirac semimetal Cd_3As_2 , where spin-orbit coupling is more important than electron-electron interaction. A qualitatively similar kind of behaviour has been predicted using the renormalization group analysis [29]. In that work, the authors have claimed that a quantum phase transition in 3D Dirac semimetals occurs due to the fascinating interplay of Coulomb interaction and disorder. The

non-Fermi liquid ground state can be achieved by increasing the strength of disorder. This theoretical study is consistent with our observation. It seems that B is playing the role of disorder in the present study. As another possible explanation, the field-induced violation of conventional WFL may be an interesting property of topological Fermi-liquid [30](Landau Fermi-liquid including Berry's phase in presence of broken inversion or time-reversal symmetry), which is unexplored till now. A quadratic B dependence of Lorentz number has been theoretically predicted for Weyl semimetal [31] (which is also a topological Fermi-liquid system), due to the chiral anomaly. Further theoretical studies are necessary to understand the possible origin of such a strong violation of WFL.

Methods

Single crystals of Cd_3As_2 were synthesized by chemical vapor transport technique [28]. Powder X-ray diffraction of crashed single crystals shows that these crystals have I_{41}/acd space group and contain no impurity phases [28]. The Cd_3As_2 single crystal was cut and polished to a bar shape, with dimension $\sim 3 \times 2 \times 0.6 \text{ mm}^3$ for transport measurements. The resistivity, thermal conductivity and thermoelectric power (Seebeck coefficient) measurements on Cd_3As_2 single crystals were done by four-probe technique in a physical property measurement system (Quantum Design) upto 9 T. Though several single crystals have been studied, we present the data for a single crystal as a representative. Qualitative similar behavior has been observed for other crystals. Creating a temperature gradient along the current direction, the measurements were performed by applying magnetic field perpendicular to them.

References

1. Wang, Z. J., Sun, Y., Chen, X. Q., Franchini, C., Xu, G., Weng, H. M., Dai, X., and Fang, Z. Dirac semimetal and topological phase transitions in A_3Bi ($\text{A} = \text{Na, K, Rb}$). *Phys Rev B* **85**, 195320 (2012).
2. Wang, Z., Weng, H., Wu, Q., Dai, X. & Fang, Z. Three-dimensional Dirac semimetal and quantum transport in Cd_3As_2 . *Phys. Rev.B* **88**, 125427 (2013).
3. Liu, Z. K., Zhou, B., Zhang, Y., Wang, Z. J., Weng, H. M., Prabhakaran, D., Mo, S.-K., Shen, Z. X., Fang, Z., Dai, X., Hussain, Z. & Chen, Y. L. Discovery of a Three-Dimensional Topological Dirac Semimetal, Na_3Bi . *Science* **343**, 864 (2014).
4. Xu, S. -Y., Liu, C., Kushwaha, S. K., Chang, T. -R., Krizan, J. W., Sankar, R., Polley, C. M., Adell, J., Balasubramanian, T., Miyamoto, K., Alidoust, N., Bian, G., Neupane, M., Belopolski, I., Jeng, H. -T., Huang, C. -Y., Tsai, W. -F., Lin, H., Chou, F. C., Okuda, T., Bansil, A., Cava, R. J. & Hasan, M. Z. Observation of a bulk 3D Dirac multiplet, Lifshitz transition, and nested spin states in Na_3Bi . *Science* **347**, 294 (2015).
5. Liu, Z. K., Jiang, J., Zhou, B., Wang, Z. J.,

- Zhang, Y., Weng, H. M., Prabhakaran, D., Mo, S. -K., Peng, H., Dudin, P., Kim, T., Hoesch, M., Fang, Z., Dai, X., Shen, Z. X., Feng, D. L., Hussain, Z. & Chen, Y. L. A stable three-dimensional topological Dirac semimetal Cd_3As_2 . *Nat. Mater.* **13**, 677 (2014).
6. Neupane, M., Xu, S. -Y., Sankar, R., Alidoust, N., Bian, G., Liu, C., Belopolski, L., Chang, T. -R., Jeng, H. -T., Lin, H., Bansil, A., Chou, F. & Hasan, M. Z. Observation of a three-dimensional topological Dirac semimetal phase in high-mobility Cd_3As_2 . *Nat. Commun.* **5**, 3786 (2014).
7. Borisenko, S., Gibson, Q., Evtushinsky, D., Zabolotnyy, V., Büchner, B. & Cava, R. J. Experimental Realization of a Three-Dimensional Dirac Semimetal. *Phys. Rev. Lett.* **113**, 027603 (2014).
8. Young, S. M., Zaheer, S., Teo, J. C. Y., Kane, C. L., Mele, E. J. & Rappe, A. M. Dirac Semimetal in Three Dimensions. *Phys. Rev. Lett.* **108**, 140405 (2012).
9. Mănes, J. L. Existence of bulk chiral fermions and crystal symmetry. *Phys. Rev. B* **85**, 155118 (2012).
10. Pfau, H., Hartmann, S., Stockert, U., Sun, p., Lausberg, s., Brando, m., Friedemann, s., Krellner, C., Geibel, C., Wirth, s., Kirchner, s., Abrahams, E., Si, Q. & Steglich, F. Thermal and electrical transport across a magnetic quantum critical point. *Nature* **484**, 493-497 (2012).
11. Grigera, S. A. et al. Magnetic field-tuned quantum criticality in the metallic ruthenate $\text{Sr}_3\text{Ru}_2\text{O}_7$. *Science* **294**, 329-332 (2001).
12. Castro Neto, A. H., Peres, N. M. R., Novoselov, K. S. & Geim, A. K. The electronic properties of graphene. *Rev. Mod. Phys.* **81**, 109(2009).
13. Hasan, M. Z. & Kane, C. L. *Colloquium: Topological insulators*. *Rev. Mod. Phys.* **82**, 3045 (2010).
14. Qi, X. -L. & Zhang, S. -C. Topological insulators and superconductors. *Rev. Mod. Phys.* **83**, 1057 (2011).
15. Richard, P., Nakayama, K., Sato, T., Neupane, M., Xu, Y.-M., Bowen, J. H., Chen, G. F., Luo, J. L., Wang, N. L., Dai, X., Fang, Z., Ding, H. & Takahashi, T. Observation of Dirac Cone Electronic Dispersion in BaFe_2As_2 . *Phys. Rev. Lett.* **104**, 137001 (2010).
16. He, L. P., Hong, X. C., Dong, J. K., Pan, J., Zhang, Z., Zhang, J. & Li, S. Y. Quantum Transport Evidence for the Three-Dimensional Dirac Semimetal Phase in Cd_3As_2 . *Phys. Rev. Lett.* **113**, 246402 (2014).
17. Potter, A. C., Kimchi, I., & Vishwanath, A. Quantum oscillations from surface Fermi arcs in Weyl and Dirac semimetals. *Nature Communications* **5**, 5161 (2014).
18. Liang, T., Gibson, Q., Ali, M. N., Liu, M., Cava, R. J. & Ong, N. P. Ultrahigh mobility and giant magnetoresistance in the Dirac semimetal Cd_3As_2 . *Nat. Mater.* **14**, 280 (2015).
19. Feng, J., Pang, Y., Wu, D., Wang, Z., Weng, H., Li, J., Dai, X., Fang, Z., Shi, Y. & Luyar, L. Large linear magnetoresistance in Dirac semi-metal Cd_3As_2 with Fermi surfaces close to the Dirac points, *arXiv:1405.6611*.
20. Gegenwart, P. et al. Magnetic-field induced quantum critical point in YbRh_2Si_2 . *Phys. Rev. Lett.* **89**, 056402 (2002).
21. Korenblit, L. L. & Sherstobitov, V. E. Electron scattering insb-type semiconductors. *Soviet physics-semiconductors* **2**, 564 (1968).
22. Armitage, D. & Goldsmid, H. J. The thermal conductivity of cadmium arsenide. *J. Phys. C*, VOL. 2, 2138 (1969).
23. Lukas, K. C., Liu, W. S., Joshi, G., Zebajjadi, M., Dresselhaus, M. S., Ren, Z. F., Chen, G., & Opeil, C. P. Experimental determination of the Lorenz number in $\text{Cu}_{0.01}\text{Bi}_2\text{Te}_{2.7}\text{Se}_{0.3}$ and $\text{Bi}_{0.88}\text{Sb}_{0.12}$. *Phys. Rev. B* **85**, 205410 (2012).
24. Jacoboni, C. *Theory of Electron Transport in Semiconductors* (Springer, Berlin, 2010).
25. Lundgren, R., Laurell, P. & Fiete, G. A. Thermoelectric properties of Weyl and Dirac semimetals. *Phys. Rev. B* **90**, 165115 (2014).
26. Jin, H., Restrepo, O. D., Antolin, N., Boona, S. R., Wind, W., Myers, R. C., and Heremans, J. P. Phonon-induced diamagnetic force and its effect on the lattice thermal conductivity. *Nat. Mater.* **14**, 601-606 (2015).
27. Hwang, E. H., Rossi, E. & Das Sarma, S. Theory of thermopower in two-dimensional graphene. *Phys. Rev. B* **80**, 235415 (2009).
28. Pariari, A., Dutta, P. & Mandal, P. Probing the Fermi surface of three-dimensional Dirac semimetal Cd_3As_2 through the de Haasvan Alphen technique. *Phys. Rev. B* **91**, 155139 (2015).
29. Moon, E.- G. & Kim, Y. B. Non-Fermi Liquid in Dirac Semi-metals. *arXiv:1409.0573*.
30. Haldane, F. D. M. Berry Curvature on the Fermi Surface: Anomalous Hall Effect as a Topological Fermi-Liquid Property. *Phys. Rev. Lett.* **93**, 206602 (2004).
31. Kim, K-S. Role of axion electrodynamics in a Weyl metal: Violation of Wiedemann-Franz law. *Phys. Rev. B* **90**, 121108(R) (2014).

Acknowledgement: We thank A. Midya, and A. Paul for their help during measurements and useful discussions.

Supplementary information for "Magnetic field induced drastic violation of Wiedemann-Franz law in Dirac semimetal Cd₃As₂"

I. TEMPERATURE DEPENDENCE OF SEEBECK COEFFICIENT (S) UNDER APPLICATION MAGNETIC FIELD (B).

Figure 6 shows linear T dependence of S both in presence and absence of external magnetic field (B) upto 350K. This implies Mott's semiclassical formula of thermoelectric power also holds in presence of B . So the expression, $S = \frac{\pi^2 k_B}{3e} \frac{k_B T}{E_F} (m + 2)$, can be used to calculate the B dependence of scattering exponent (m).

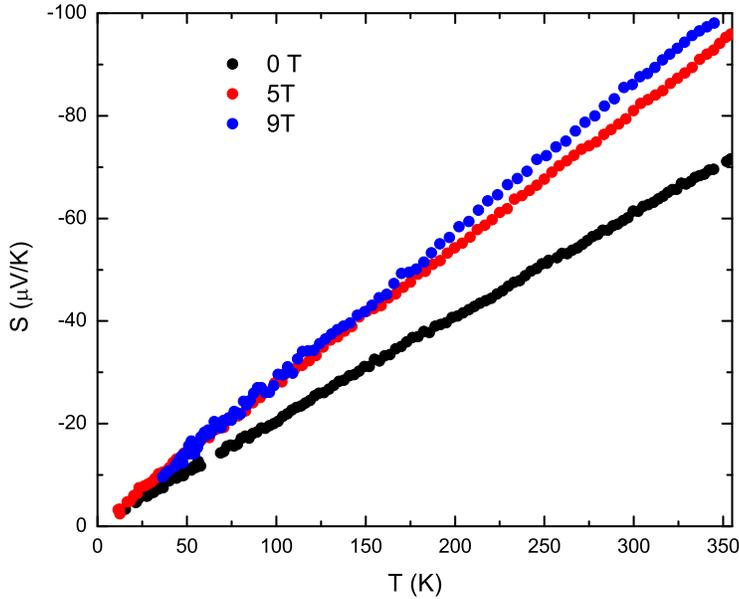


FIG. 6: (Color online) Temperature dependence of S at 0T, 5T and 9T magnetic field.